Supplement of Atmos. Chem. Phys., 18, 11739–11752, 2018
https://doi.org/10.5194/acp-18-11739-2018-supplement

Atmospheric Chemistry and Physics
Open Access
EGU

Supplement of

Characterization of aerosol hygroscopicity, mixing state, and CCN activity at a suburban site in the central North China Plain

Y. Wang et al.

Correspondence to: Zhanqing Li (zli@atmos.umd.edu)

Table S1. Gravimetric densities (ρ) and hygroscopicity parameters (κ) used in this study.

Species	NH_4NO_3	$(NH_4)_2SO_4$	NH_4HSO_4	H_2SO_4	POA	SOA	BC
ρ (kg m^{-3})	1720	1769	1780	1830	1000	1400	1700
κ	0.67	0.61	0.61	0.9	0	0.1	0

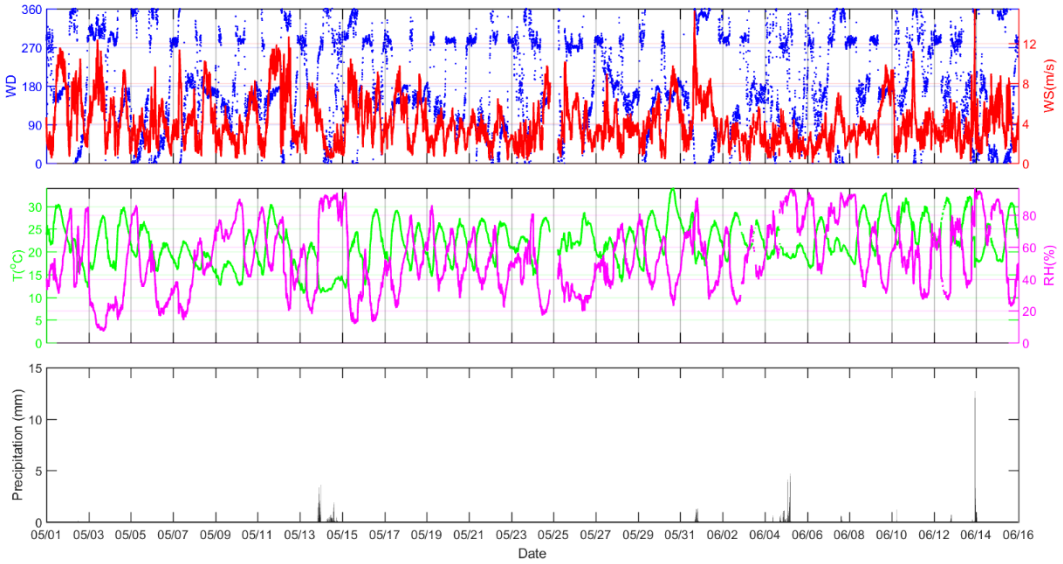

Figure S1. Time series of different meteorological variables measured at the site: wind direction (WD), wind speed (WS), ambient temperature (T), relative humidity (RH), and the amount of precipitation.

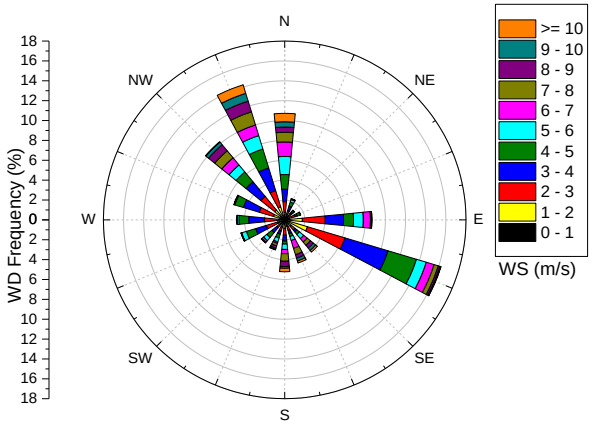

Figure S2. Wind rose diagram summarizing wind directions (WD) and wind speeds (WS) during the measurement period.

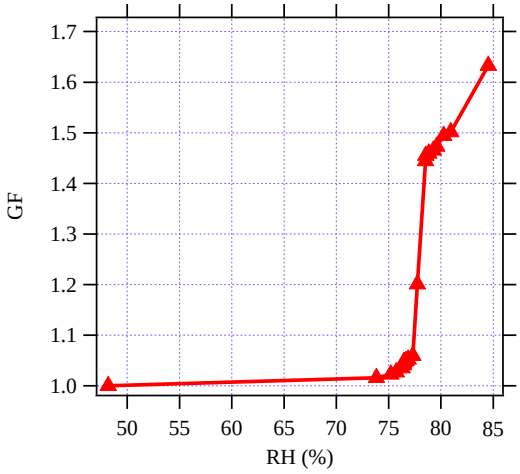

Figure S3. Humidogram of ammonium sulfate for 150-nm particles measured with HTDMA during this campaign.

The RH calibration is important for HTDMA running, especially for high RH measurement. Figure S3 shows the calibration result with ammonium sulfate during this campaign. It shows the deliquescence point of ammonium sulfate is 78±1 %, this is consistent with previous studies (Badger et al., 2006; Tan et al., 2013).

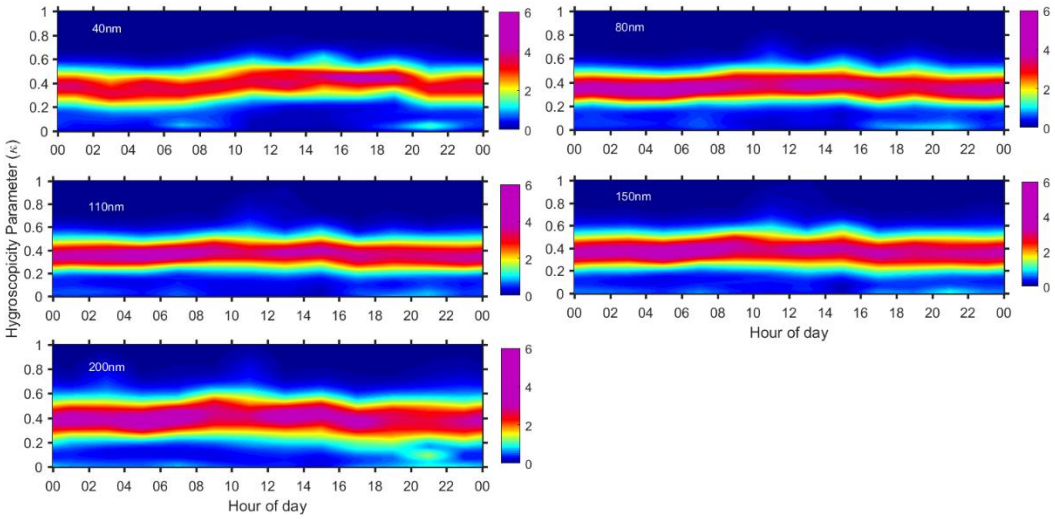

Figure S4. Diurnal variations in the probability density functions of κ_{gf} (κ-PDF) for different particle sizes.

Figure S4 shows the diurnal variations in κ-PDF for different particle sizes. Unimodal distributions were always seen. Two or three modes occasionally appeared at night. This is likely because photochemical reactions were weak at night and the newly effluent hydrophobic species (such BC and organics) cannot quickly mix with inorganic salts.

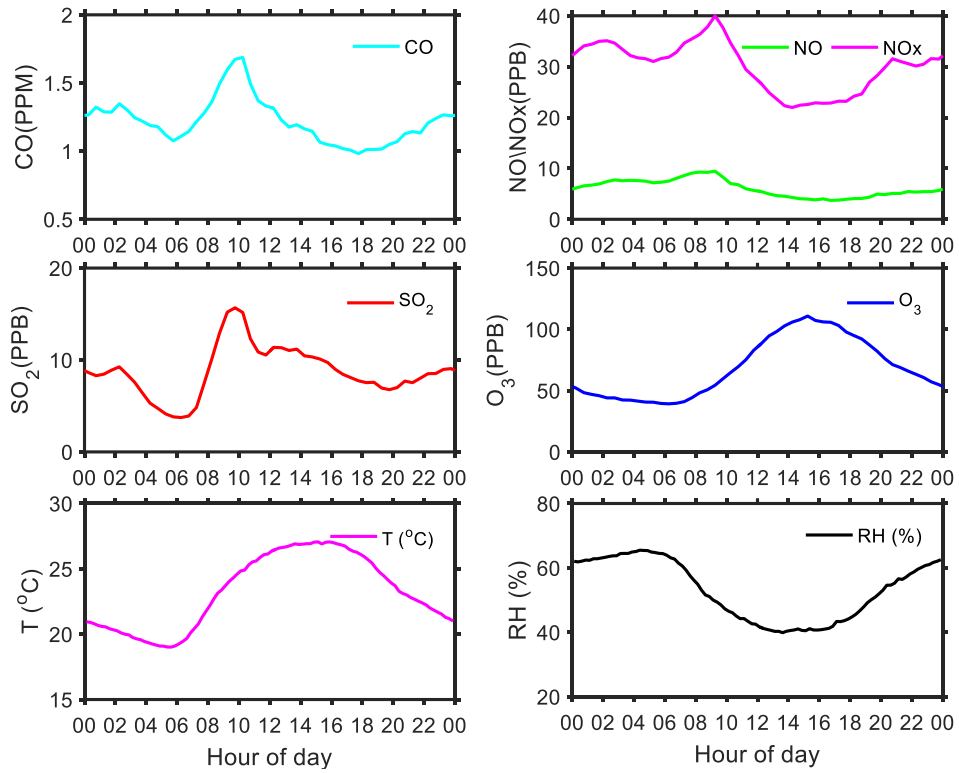

Figure S5. Diurnal variations in trace gases (CO, NOx/NO, SO_2 and O_3) and meteorological variables (*T* and RH).

Figure S5 shows the diurnal variations in trace gases and meteorological variables. Affected by the mountain-valley wind, prevailing winds shifted from the northwest to the southeast in the early morning. There are more industrial emissions to the southeast of the measurement site than to the northwest of the site. Therefore, the CO and SO_2 concentrations increased sharply in the morning after the wind shifted. The increased CO suggests the increase of VOCs because of their similar sources. The O_3 concentration increased gradually after sunrise during the day, reflecting the enhancement of atmospheric oxidation capacity. The ample supply of effluent SO_2 and VOCs precursors and the strong atmospheric oxidation capacity under high RH and low *T* conditions made plenty of sulfate and SOA produced (Wang et al., 2016; Wang et al., 2017). This is the reason in the frequent occurrence of NPF events and

the enhancement of aerosol hygroscopicity during the daytime at XT.

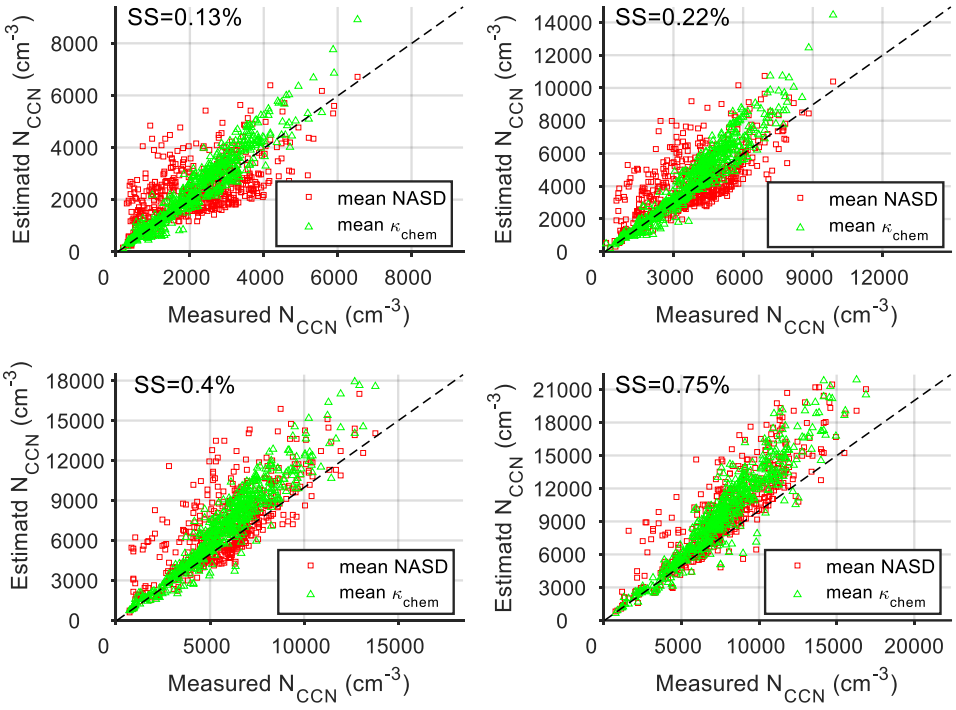

Figure **S6**. Correlation of the actual CCN number concentration time series with an estimated time series using mean NASD (normalized aerosol size distribution) but variable composition (κchem) or using mean κchem but variable NASD.

Figure S6 depicts the sensibility tests of aerosol size distribution and chemical composition to the CCN number concentration estimation, which is similar with that of Dusek et al., (2006). The figure shows the correlation using mean NASD was weaker than that using mean κchem, reflecting the more important effect of particle size for aerosol CCN activity than chemical composition.

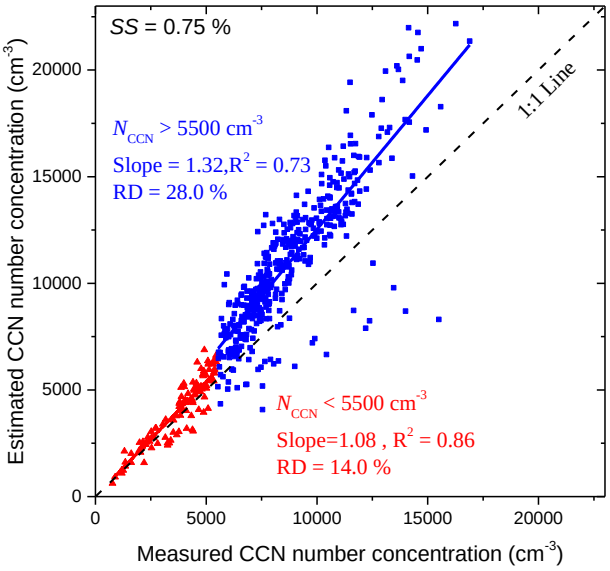

Figure S7. Estimated versus measured CCN number concentrations at SS = 0.75 % (corresponding to Fig. 9-a4 in the paper). The N_{CCN} is estimated based on κ-Köhler theory, using the real-time κ_{chem}. Here, the critical value of N_{CCN} = 5500 cm^{-3} is used to separate the points into two groups. A separate linear regression analysis is done on each group. The slopes, correlation coefficients (R^2), and relative deviations (RD) are shown in the figure.

Figure S7 shows that the linear regression is better when N_{CCN} < 5500 cm^{-3}. The slope and RD for N_{CCN} < 5500 cm^{-3} are much lower than the values calculated using all N_{CCN} data (section 4.4 in the paper), while the values for N_{CCN} > 5500 cm^{-3} are higher. This suggests that the CCN deviations are mainly caused by the overestimation of N_{CCN} due to measurement uncertainties (section 4.4). The good closure when N_{CCN} < 5500 cm^{-3} also reflects the closure method used in this study is valid.

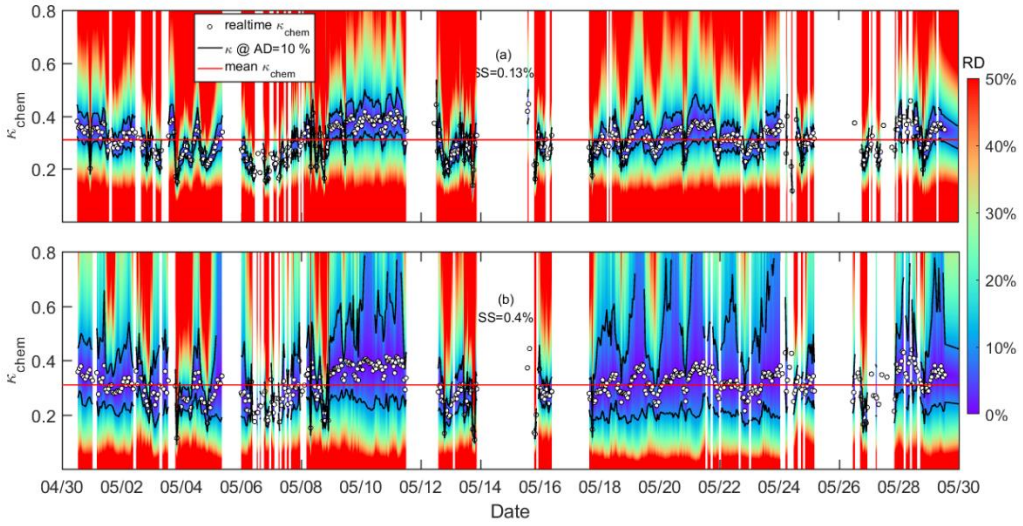

Figure S8. Sensitivity of N_{CCN} estimates to κ_{chem} as a function of time at (a) SS = 0.13 % and (b) SS = 0.40 %. More information about the plot can be found in the Fig. 9 caption.

References:

Badger C.L., George I., Griffiths P.T., Braban C.F., Cox R.A. and Abbatt J.P.D.: Phase transitions and hygroscopic growth of aerosol particles containing humic acid and mixtures of humic acid and ammonium sulphate, Atmos Chem Phys, 6, 755-768, https://doi.org/10.5194/acp-6-755-2006, 2006.

Dusek U., Frank G.P., Hildebrandt L., Curtius J., Schneider J., Walter S., Chand D., Drewnick F., Hings S. and Jung D.: Size matters more than chemistry for cloud-nucleating ability of aerosol particles, Science, 312, 1375-8, https://doi.org/10.1126/science.1125261, 2006.

Tan H., Xu H., Wan Q., Li F., Deng X., Chan P.W., Xia D. and Yin Y.: Design and application of an unattended multifunctional H-TDMA system, J. Atmos Ocean Tech, 30, 1136-1148, https://doi.org/10.4209/aaqr.2017.01.0020, 2013.

Wang G., Zhang R., Gomez M.E., Yang L., Zamora M.L., Hu M., Lin Y., Peng J., Guo S. and Meng J.: Persistent sulfate formation from London Fog to Chinese haze, Proceedings of the National Academy of Sciences, 113, 13630-13635, https://doi.org/10.1073/pnas.1616540113, 2016.

Wang Z., Wu Z., Yue D., Shang D., Guo S., Sun J., Ding A., Wang L., Jiang J. and Guo H.: New particle formation in China: Current knowledge and further directions, Sci Total Environ, 577, 258-266, https://doi.org/10.1016/j.scitotenv.2016.10.177, 2017.